Journal of Hydrology 593 (2021) 125808

Contents lists available at ScienceDirect

Journal of Hydrology

journal homepage: www.elsevier.com/locate/jhydrol

Research papers

Hydrological benefits of restoring wildfire regimes in the Sierra Nevada persist in a warming climate

Ekaterina Rakhmatulina [a,*], Gabrielle Boisramé [a,b], Scott L. Stephens [d], Sally Thompson [a,c]

[a] Department of Civil and Environmental Engineering, University of California, Berkeley, CA, USA
[b] Division of Hydrologic Sciences, Desert Research Institute, Las Vegas, Nevada, USA
[c] Department of Environmental Engineering, University of Western Australia, WA, Australia
[d] Department of Environmental Science, Policy, and Management, University of California, Berkeley, CA, USA

A B S T R A C T

Reducing the risk of wildfire and increasing the security of water supply from mountain catchments are both urgent priorities in the Western US. These goals may be synergistic, thanks to the reductions in transpiration and fire hazard associated with reducing forest cover. Data and modeling efforts based on the Illilouette Creek Basin (ICB) in Yosemite National Park, where fire use policies have been implemented to restore wildfire since 1972, suggest that these policies reduced fire hazards and increased annual streamflow production through large changes to landscape-scale forest cover and structure. Expanding fire use strategies through the Western US, however, would mean that any such changes in forest cover and structure would occur in the middle of the 21st century, under different fire frequency and climate conditions than experienced in the ICB to date. It is therefore important to understand if hydrological benefits of fire use are sensitive to anticipated changes in climate and fire frequency. Here, we force an ecohydrological model previously developed for the ICB with an ensemble of downscaled future climate predictions to assess the impacts of climate change and fire use strategies on the hydrology of the ICB. We find that the hydrological impacts of fire use are comparable under observed climate and projected future climates, and are largely insensitive to the significant uncertainties regarding post-fire successional trajectories for vegetation. While expected increases in fire frequency cause minor changes in the basin hydrology, the main impact of more frequent fires is to cause the basin to reach peak hydrological change more rapidly.

1. Introduction

Mountain watersheds represent a locus of environmental change and vulnerability in the Western US. The Sierra Nevada, for example, produce 9–30% of California's electricity, and 60–90% of California's water supply (Madani and Lund, 2009), "provisioning" ecosystem services (Stephens et al., 2020) that supply water to 30 million of the state's residents and support agricultural industries with an estimated value of $50 billion/year (Klausmeyer and Fitzgerald, 2012; California Department of Food and Agriculture, 2019). These watersheds, however, experience a naturally volatile climate, are expected to warm and dry due to climate change, and are at increasing risk of disturbance, particularly from wildfire, which is also expected to increase in severity and frequency in a warmer climate (Goulden and Bales, 2019; Westerling, 2008). This volatility, warming, drying, and increase in fire risk present significant risks to power production (Tarroja et al., 2016), water supply (Dahm et al., 2015; Writer et al., 2014), human lives (CalFire, 2019a), health and infrastructure (CalFire, 2019b), biodiversity (Richter et al., 2019), ecosystem services (Wood and Jones, 2019), and amenity of the montane landscape (Millar and Stephenson, 2015). Conventional management approaches are unlikely to be able to address these joint threats: for example, the costs of fire suppression and fire-fighting in California are growing exponentially, reaching $950 million USD in 2018 (CalFire, 2019c) with reparation costs in the billions of dollars (Thomas et al., 2017).

Consequently, foresters and catchment managers are seeking alternative management paradigms for fire-prone montane forests (Stephens et al., 2020). One option is to adopt a "fire use" policy, also known as "managed wildfire", for watershed management. Fire use policies allow lightning-ignited wildfires to burn, subject to a strict management policy that calls for intervention to suppress fire when air quality, structures, or people are placed at risk (van Wagtendonk, 2007). In part, this policy attempts to restore the natural fire-regime in Western US forests, reversing the more than one hundred years of fire suppression in the region. Fire suppression has altered contemporary forests relative to their pre-European settlement condition, such that fuel loads, the prevalence of shade-tolerant and fire-intolerant species, and density of forest vegetation have all increased relative to historical baselines (Collins and Stephens, 2007; van Wagtendonk et al., 2012; Scholl and Taylor, 2010; Stephens et al., 2015). Although interest in adopting fire

* Corresponding author.
E-mail address: erakhmat@berkeley.edu (E. Rakhmatulina).

https://doi.org/10.1016/j.jhydrol.2020.125808
Received in revised form 4 November 2020; Accepted 23 November 2020
Available online 8 December 2020

use strategies is growing (Stephens et al., 2016), there have been relatively few locations where they have been implemented for long enough to assess their effects. Within the Sierra Nevada, the Illilouette Creek Basin (ICB) in Yosemite National Park, CA (Collins and Stephens, 2007), has experienced 29 fires larger than 40 ha since 1972, when 100 years of fire exclusion and suppression in the Basin ended (van Wagtendonk et al., 2012). ICB is located in proximity to long-term weather stations and is gauged shortly downstream of its confluence with the Upper Merced River. These unique characteristics have made it the subject of ongoing research to establish the ecological and hydrological effects of fire use policies (e.g. Collins and Stephens, 2007; Ponisio et al., 2016; Boisramé et al., 2017a, 2018, 2019).

Hydrologically, the impact of fire use strategies in the ICB has been to increase streamflow production and expand wet environments (Boisramé et al., 2017a, 2019). Changes to the water balance of the basin inferred using the Regional Hydro-Ecological Simulation System (RHESSys) suggest that annual transpiration has decreased by up to 30 mm, peak snowpack depth increased by up to 10 mm of snow water equivalent (SWE), annual discharge has increased by up to 40 mm/year in the fire-affected section of the watershed or approximately 5% (25 mm/year) overall, and storage of water in the soil and groundwater (referred to as subsurface storage hereafter) has increased by an average of 60 mm (Boisramé et al., 2019). These changes, although modest, are comparable to inference of increased streamflow, subsurface storage and snowpack, and decreased evapotranspiration, following wildfires in the Consumnes Watershed in the Sierra Nevada (Maina and Siirila-Woodburn, 2019). Such post-fire wetting occurs against a background of warming and drying in the Sierra Nevada, and could represent a positive hydrological co-benefit relevant to the social and economic case for fire-use policies (c.f. González-Sanchis et al., 2019).

Expanding wildland fire use policies to other locations involves confronting the long timescales on which the forests adjust to changed fire regimes (Stevens et al., 2020). These timescales mean that changes in fire management policy implemented in the near future would impact forests and their hydrology during the mid-21st century, in comparison to the late 20th century when most of the changes occurred in the ICB. Thus, before attempting to use the hydrological insights gained from the ICB to inform contemporary forest management decisions, it is pertinent to ask whether the hydrological outcomes of wildland fire use are sensitive to the changes in climate expected by the mid-21st century. Although assessments of the hydrological impact of climatic extremes on watersheds in the Western US suggest that the increases in streamflow due to wildfire dwarf the reductions predicted due to climate change by 2050 (Wine et al., 2018), many uncertainties surround these predictions, including variable effects of post-fire vegetation growth rates and the impact of different fire regimes on water balance (Tague et al., 2019), poorly understood post-fire vegetation successional trajectories in a changed climate, and uncertainties surrounding the future fire regime itself.

By the mid-21st Century, the Sierra Nevada region is projected to be warmer, to experience similar or slightly elevated precipitation inputs (Dettinger, 2005; Pierce et al., 2013), and more frequent fires than in the 1972-present period (Westerling, 2008; Yue et al., 2013; Geos Institute, 2013). Multiple studies agree that warmer conditions will dry fuels and increase fire frequency, severity, and extent (e.g. Westerling, 2008, 2018; Littell et al., 2009), but recent re-appraisals of this work in the Sierra Nevada suggest that fire frequency in future climates is overestimated because projections have ignored the effects of fuel limitation (Hurteau et al., 2019). Additional complexities, including non-stationary relationships between drought and fire occurrence across climate gradients (McKenzie and Littell, 2017), and feedbacks between fire extent, vegetation dynamics and distributions (Syphard et al., 2018), mean there is considerable uncertainty regarding the future fire regime; so much that Syphard et al. (2018) concluded that there was "no way to ascertain which projections of fire are most feasible".

Compounding uncertainties about future fire regimes is the hard-to-predict successional trajectory of vegetation post-fire, and the interaction of these trajectories with a non-stationary climate (Lenihan et al., 2003; Steel et al., 2015; Cornwell et al., 2012; Batllori et al., 2015). Rapid vegetation transitions from conifer forests to shrubland are associated with the loss of tree seed banks, which limits forest regeneration within large patches of high severity fire (Meng et al., 2015; Young et al., 2019), and with arid post-fire conditions that create unfavorable growth conditions for many forest species (Davis et al., 2019). Shrublands regenerate rapidly after a fire and have a greater tolerance for arid conditions (Lauvaux et al., 2016; Serra-Diaz et al., 2018; Baudena et al., 2019). In the absence of high severity fires, forest succession occurs on timescales of multiple decades (Halofsky et al., 2018; Liang et al., 2016), and fire excluded forests are hypothesized to lie near tipping points where disturbances could cause significant changes in vegetation composition (Batllori et al., 2018). This literature suggests that the potential range of post-fire vegetation transitions is poorly bounded.

Fully predicting the effects of wildland fire use on hydrologic regimes under future climates would require unraveling these uncertain processes to specify the feedbacks between vegetation, water, fire risk and successional dynamics, a highly challenging problem (Brotons and Duane, 2019; Riley et al., 2019). We therefore do not directly address this problem for the specific case of the ICB, but instead adopt a set of simplifying assumptions which are further developed and justified in the methods section: (i) we use standard approaches to predicting future climate in ICB by downscaling and bias correction of an ensemble of global circulation models (Lanzante et al., 2019; Luo et al., 2018), (ii) we assume that the characteristics of the fire regime that would arise if applied to fire-suppressed forests in 2030–2070 are well represented by the severity – area distribution of the historical fires that occurred in ICB from 1972–2010, and we allow for the frequency of these fires to increase across a set of scenarios drawn from the literature and considering climate impacts on frequency only (see Section 2.4 for details). Specifically, the assumptions keep severity and fire area constant, and therefore do not account for possible feedbacks between these aspects of fire, climate, and vegetation. Finally (iii) we assess the hydrological implications of climate change on fire impacts under two vegetation scenarios: one in which post-fire vegetation transitions match those which occurred in the historical period (a scenario which might arise if, for example, topography and geological context primarily drive vegetation community types), and one "bounding case" scenario in which we force all post-fire vegetation regeneration to occur as a single plant type (conifers, shrublands, or wet meadows), assuming that reality would lie in between these extreme limits of vegetation change. With these assumptions, we use an existing RHESSys model parameterization for the ICB (Boisramé et al., 2019) to answer three questions:

i) How would the hydrology of the ICB respond to climate change in the absence of the fire use policy, where vegetation remains in a fire excluded state?

ii) How do the hydrological outcomes of fire use strategies in ICB differ under future climate conditions (2030–2070; RCP 4.5 and RCP 8.5), relative to those outcomes under the observed climate (1970–2010)?

and

iii) How sensitive are the hydrological outcomes of fire use strategies for the 2030–2070 period to potential increases in fire frequency?

2. Methods

2.1. Study site

Illilouette Creek Basin (ICB) is located within Yosemite National Park, California, USA (Fig. 1). The 150 km^2 basin spans an elevation range of 1,270–3,600 meters, with a mean elevation of 2,500 meters. About 41% of the ICB is forested with *Pinus jeffreyi*, *Abies concolor*, *Abies magnifica*, and *Pinus contorta*, interspersed with meadows (16%) and

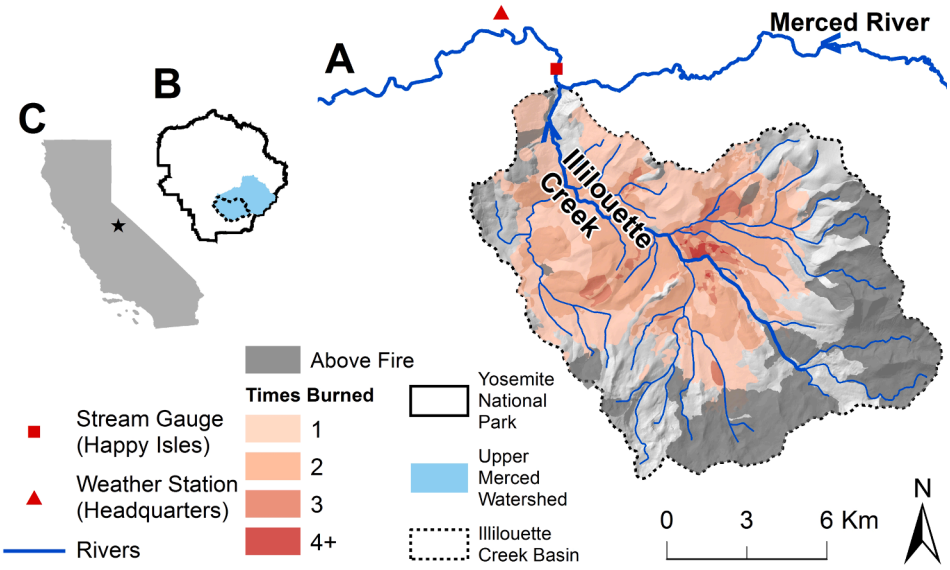

Fig. 1. Study site location: Illilouette Creek Basin (A), within Yosemite National Park (B), California (C). Stream gauging station (Happy Isles) and weather station are displayed along with major rivers and tributaries.

shrubland (9%). About 34% of the basin is high elevation granite, which acts to confine fires to the basin (Boisramé et al., 2017b; Collins et al., 2009).

ICB experiences a Mediterranean climate with warm dry summers and cool wet winters. The nearest weather station is located in Yosemite Valley (1,240 meters, 37.74 lat, −119.59 lon, CDEC station YYV), and has operated since 1926. Over 1970–2010, this station recorded a mean annual precipitation of 92.0 cm, mean daily minimum January temperature of −2 °C and mean daily maximum July temperature of 27 °C. The ICB has similar precipitation totals to Yosemite Valley, but is approximately 7 °C cooler (January 2015 to December 2017, Appendix Fig. B.1), leading to a greater fraction of precipitation falling as snowfall. While streamflow data for the ICB itself are limited, the basin comprises 33% of the Upper Merced River Basin, which has a century-long streamflow record at the Happy Isles gauge located downstream of the confluence of the Illilouette Creek with the Upper Merced River (Fig. 1; Boisramé et al., 2019). The mean flow at Happy Isles was 10 m^3/sec (71 cm/year) for 1970–2010 (USGS gauge # 11264500, data from waterdata.usgs.gov).

During the period from 1700–1900, prior to fire suppression, ICB had a fire return interval of 6.3 years. Following the initiation of fire use strategies, the fire return interval was 6.8 years (from 1972–2005), similar to the pre-exclusion era (Collins and Stephens, 2007). From 1972 to 2019, there were 29 fires greater than 40 ha in ICB, of which 1 was human caused (1986, burned 291 ha), 1 was prescribed (1999, 54 ha), and the other 27 fires were lightning ignited (van Wagtendonk et al., 2012). Of the 8187 ha burned in ICB (75% of the watershed's vegetated area), 4463 ha (55%) burned twice, 767 ha (9%) three times, 72 ha (1%) four times, and 4 ha (<1%) five times (Fig. 1). As shown in Fig. 2, this high wildfire activity in ICB has doubled the area of dense and sparse meadows in the basin (Boisramé et al., 2017b, 2018), increased landscape heterogeneity and habitat for multiple plant and animal species, and is associated with increased biodiversity (Ponisio et al., 2016; Campos et al., 2017; Stephens et al., 2019).

The contemporary (1972-present) fire regime in the ICB has been relatively stationary (Fig. 3). Following the initiation of fire use

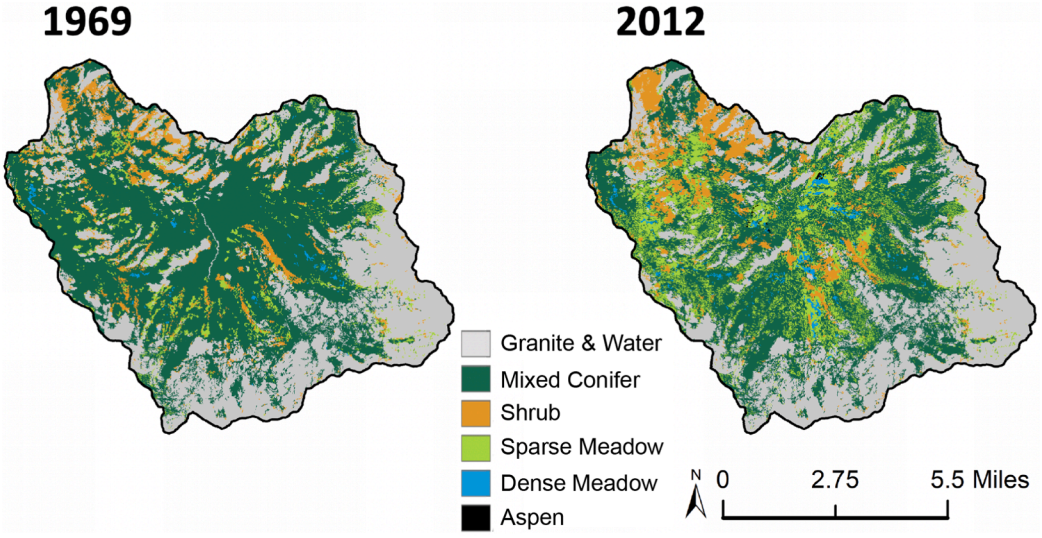

Fig. 2. Vegetation classification of ICB based on satellite imagery for 1969 (left) and 2012 (right). 1969 landscape signifies over 100 years of fire suppression, while 2012 represents 40 years of fire use strategies.

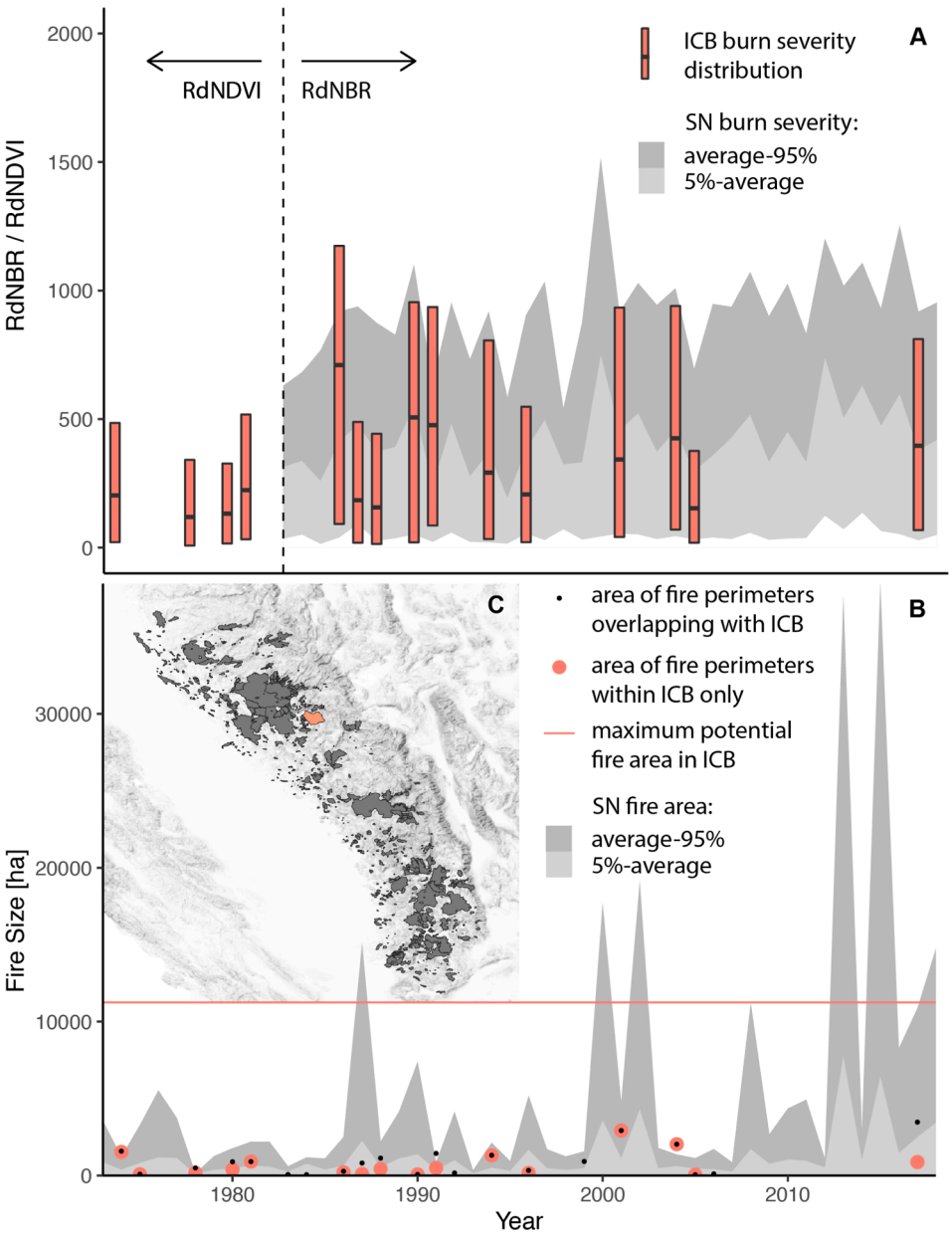

Fig. 3. Burn severity for fires that occurred within ICB (red in C) and the surrounding Sierra Nevada (SN) region (SN fires are dark gray in C) were assessed using Landsat-derived RdNBR index for years after 1983 and RdNDVI prior to 1983 (A). For the SN, a 90% confidence interval is provided along with the average fire size for the years 1984–2018. Fire severity in ICB is shown as a box and whisker plot in red, where the range is the 5th through 95th percentile, and the average is shown as a horizontal dash. In B, mean and 90th percentile fire size from 1974–2018 is shown for fires in the SN (gray colors). Red dots in B are fire areas within the ICB only, and black dots are full fire perimeters of which at least a portion was within the ICB. The maximum fire size within ICB (vegetated area of ICB) is shown as a horizontal red line. Fires less than 40 hectares were excluded from both the SN and ICB analyses. (For interpretation of the references to color in this figure legend, the reader is referred to the web version of this article.)

strategies, the fires were relatively small in area with low to moderate burn severities, as assessed by Landsat-derived indices, where the Relative difference Normalized Vegetation Index (RdNDVI) was used prior to 1984, and the Relative difference Normalized Burn Ratio (RdNBR) post 1984 (Collins et al., 2009). Both burn severities (Fig. 3-A) and burn areas (Fig. 3-B) in the ICB are more stable in the contemporary period than in the surrounding Sierra Nevada, where fire severity and area have both increased. Fire perimeters in the ICB indicate that fires in the basin are self-limiting (Collins et al., 2009).

2.2. RHESSys model

The Regional Hydro-Ecological Simulation System (RHESSys, version 5.20.1) is a spatially distributed ecohydrological model that simulates water, energy, and vegetation growth processes. It represents landscapes through a hierarchy of spatial units: small areas of uniform soil and vegetation are represented as patches, water is routed between patches within hillslopes, and basin-scale processes arise from water fluxes and stores aggregated across hillslopes. The ability of RHESSys to simulate climatic, hydrological and vegetation growth processes at a basin scale makes it well suited to simulating the effects of disturbance (such as fire) on water balance.

At the patch scale, RHESSys resolves a detailed vertical energy and water balance. The energy balance is forced by shortwave radiation inputs, varied to account for slope, aspect, topographic shading, and seasonality. Other energy flux terms, and wind speeds, are attenuated through vegetation canopies as a function of leaf area index (LAI), which itself changes dynamically as the vegetation grows. Incoming precipitation is intercepted by canopy and litter layers, and is partitioned between infiltration (via Green and Ampt, 1911) and surface detention storage (which contributes to runoff if sufficiently large) at the soil surface. Vapor fluxes include evaporation or sublimation from all vertical layers, and transpiration separately computed from sunlit and shaded canopy layers, all computed using the Penman–Monteith approach (Monteith, 1965). Infiltrated water is routed between a root zone, an unsaturated and saturated zone based on Darcy relationships and soil parameters, and lateral fluxes of water between spatially explicit patches are resolved based on surface topography and calibrated

drainage parameters. In addition to specifying LAI growth rates, species-specific plant properties control maximum stomatal conductance values and their response to changing soil water. A more detailed description of the RHESSys model is provided in Tague and Band (2004).

Boisramé et al. (2019) implemented RHESSys in the ICB, drawing on LiDAR elevation data at 10 m resolution (Kane et al., 2015), a vegetation analysis (Boisramé et al., 2017a) that used aerial photos and the Yosemite National Park vegetation mapping to delineate six cover types, daily weather data from the Yosemite Headquarters Weather Station, and flow records at Happy Isles Gauge and a short flow record within the Illilouette Creek. The six cover types are conifer forest, aspen (*Populus tremuloides*), shrub (primarily *Ceanothus cordulatus*), wet meadow (dense grasses and forbs), dry grassland (sparsely vegetated areas dominated by grasses), or unvegetated (exposed rock or sand). The model was calibrated to identify behavioral parameter ensembles consisting of (i) temperature and precipitation lapse rates (ii) decay of hydraulic conductivity with depth, (iii) saturated hydraulic conductivity at the land surface, (iv) depth of hydrologically active water storage across soil and saprolite layers, (v) the proportion of saturated soil water routed directly (via preferential flow paths) to deeper groundwater stores below plant root access, and (vi) the proportion of these deeper groundwater stores draining to the stream each day. RHESSys captures spatial variations in subsurface properties across soil types by scaling them using mapped soil categories for the ICB. Calibration was performed against Happy Isles flow data and identified an ensemble of 93 behavioral parameter sets (assessed across a multi-objective set of criteria aiming to capture volume and timing of streamflow on monthly, seasonal and annual scales) that were used to constrain model uncertainty using the Generalized Likelihood Uncertainty Estimation (GLUE) approach (Beven and Binley, 1992). More details regarding the parameterization, calibration, and validation of RHESSys for the ICB are provided in Boisramé et al. (2019).

2.3. Modeling the effect of an individual fire

Individual fires in RHESSys were defined based on fire perimeter and severity maps. Fires were treated as having an instantaneous effect on vegetation biomass, on the thickness of the litter layer, and on the species-specific properties of the vegetation (to represent post-fire vegetation transitions): these factors drive subsequent hydrological responses in RHESSys. Wildfires can, however, have other hydrologically-relevant effects that were omitted from the model, including reduced albedo from charred surfaces (Burles and Boon, 2011; Gleason et al., 2013, 2019), changes in the size and distribution of canopy gaps (Stevens, 2017; Kostadinov et al., 2019; Lundquist et al., 2013), reduced soil infiltration capacity due to ash clogging or soil hydrophobicity (Neary et al., 2005; Ebel and Moody, 2020; Doerr et al., 2006), and increased erosion rates (Larsen et al., 2009). In the ICB, low-moderate severity fires are most common (rather than the high severity fires that generate persistent changes in soil properties Doerr et al., 2006), and water quality monitoring at the Happy Isles' gauge indicates no increases in turbidity or flow peaks post-fire (results not shown). The reliance of our modeling on spatially uniform daily precipitation, although necessary given lack of more resolved precipitation data for the Merced River Basin (Henn et al., 2018) would likely prevent the model from resolving surface-flow events that might arise due to soil changes. Consequently, the model, which was calibrated to optimize long timescale water balance predictions, may under-estimate peak flow occurrences, particularly immediately post-fire.

Fire severity was used to determine the degree of biomass and litter loss in each fire-affected patch. The threshold approach of Miller and Thode (2007) was used to relate RdNDVI/RdNBR observations to fire severity in ICB following Collins et al. (2009). We considered three classes of change: (i) for RdNBR and RdNDVI values between 69 and 315 (low severity), only litter stores were removed; (ii) for values between 315 and 640 (moderate severity), in addition to litter removal, plant carbon stores were reduced 50%; (iii) for values greater than 640 (high severity), all carbon and litter layers were removed within the fire perimeter. Additionally, if analysis of aerial photos indicated a change in vegetation cover type following a fire, we mapped these patches also as high severity burn areas.

Where high severity fire occurred, all above-ground vegetation carbon and litter stores were set to zero and modeled vegetation was allowed to immediately regrow dynamically. To account for the possibility of a post-fire cover-type transition, we reset the vegetation parameters in these patches to represent one of two scenarios. In one scenario, individual pixels followed the observed historical successional trajectory that occurred in the 1972–2010 setting. In the other scenario, pixels that burned at high severity were forced to regenerate with a single vegetation type: all forest, all shrub, or all wetland. This "bounding cases" scenario was used to constrain the uncertainty in the hydrological projections that arises due to unknown patterns of future post-fire regeneration, under the assumption that enforcing a single vegetation type provides a limiting case. The bounding case scenarios were run for the historical fire regime only.

2.4. Using 1972–2010 fire data to define potential future fire regimes

The characteristics of the fire regime that has prevailed in ICB since 1972 are illustrated in Fig. 3 which shows RdNDVI and RdNBR distributions, fire return interval, and area of all fires over 40 ha. Note that the most recent fire, the Empire Fire of 2017 (the only fire after 2010) is not shown on this figure. It was omitted from this study due to a lack of data about post-fire vegetation type and condition. However, as illustrated in the Appendix Section C, the Empire Fire was similar to previous fires in size and severity. These data are suggestive of a relatively stable fire regime, consistent with the self-limiting behavior of fire in the ICB.

Defining the spatial, temporal, and severity characteristics of potential future fire regime is, as the literature reviewed in the introduction suggests, inherently uncertain. In light of these uncertainties and the stability of the fire regime in the ICB over five decades of climatic and vegetation change, we use the observed fire perimeters and severity maps to define potential future fire areas and severities. With the historical fire perimeters providing some control on fuel limitation, warmer temperatures are expected to increase the probability of ignition by decreasing fuel moisture, leading to increased fire occurrence (Riley and Loehman, 2016; Westerling, 2008; Lauvaux et al., 2016). To explore the effects of changing fire frequency, we shortened the time interval (in days) between historical fires by 30% and 60% in line with predictions for the Sierra Nevada based on climatic warming (Riley and Loehman, 2016; Westerling, 2008; Lauvaux et al., 2016). This had the effect of some fire perimeter/severity combinations being imposed twice in the modeled record – for the 30% increase in fire frequency scenario ("+30%"), these were the fires from 1974 and 1978; for the 60% scenario, the fires from 1974, 1978, 1980, 1981, 1986, 1988, and 1990 were imposed twice. As can be seen visually in Fig. 3, these fires are broadly representative of the range of fires in the ICB (i.e. we did not repeat extreme cases). We checked if these increases were reasonable in light of the minimum time needed to allow fuel to build up and reburn in the ICB – estimated as approximately 9 years (Collins et al., 2009). For a 60% increase in fire frequency scenario ("+60%"), the average interval between reusing a given fire perimeter is 24 years, and the average interval between pixels reburning is 7 years, suggesting that this increase represents a reasonable fuel-limited maximum for the basin.

Using a historical fire occurrence record as a basis for increasing fire frequency can lead to a situation where a fire is predicted to occur outside the fire season (historically observed to be June-September in the ICB). If this projected timing was such that the fire occurred in the window of April 1st to October 31st (a period that we confirmed is snow-free in all modeled future climate scenarios), we allowed the fire to burn on that projected date, in line with the expected lengthening of the regional fire season (Yue et al., 2013). If, however, the projected fire

date lay outside this seasonal range, it was assigned a random date from the nearest fire season.

The approach of using historical fire perimeters to define the future fire regime omits exploration of other future fire scenarios – for example, scenarios in which the severity/area of fires changes dramatically. Using historical fire perimeters does not allow a fully comprehensive analysis of the uncertainty in hydrological predictions associated with the specific sequence of fires. It does not explore a situation in which fire frequency is reduced in the basin relative to historical conditions; although the fact that three fires were suppressed during the California Drought (2011–2016, this is likely responsible for the large fire-free interval before the Empire Fire in 2017) suggests that reduced fire frequency regime could be a possible outcome within the future climate. Given these limitations our goal is not to be predictive, but rather to determine if the hydrological responses to this sequence of historically managed fires, or to a "sped up" version of this sequence of fires, are the same as they were under historical climate conditions.

2.5. Future climate data and bias correction

Ensembles of climate model predictions are widely recognized as being essential to characterize the uncertainty surrounding future climates (Pierce et al., 2009; Hagedorn et al., 2005; Thompson, 1977). Since too few regional climate models are available over the ICB to generate such an ensemble, we downscaled the minimum and maximum temperature and precipitation output of 10 GCMs, using data from the cell (ranging from 0.75–2.8 degrees latitude and longitude) containing the ICB, for the 2030–2070 period. In selecting 10 models, we followed the recommendations of Pierce et al. (2009), who suggested that climate ensembles became stable after 5 or more models are included. The GCMs we selected were: ACCESS1.3, CanESM2, CMCC-CM, CSIRO-Mk3.6.0, GFDL-ESM2M, INM-CM4, IPSL-CM5A-MR, MIROC5, MRI-CGCM3, and NorESM1-M (Appendix Fig. B.2 provides additional descriptions of each model). These models were chosen to maximize model skill and model independence as computed by Sanderson et al. (2017), and to cover a range of predicted future climate extremes (i.e. to include models that predict both cooler/wetter futures in the region, and those that predict hotter/drier conditions). All model data were obtained from the Coupled Model Intercomparison Project Phase 5, CMIP5 (https://esgf-node.llnl.gov/projects/cmip5), and have the same initializations, realizations, and parameterization states (abbreviated as "r1i1p1" in CMIP5). We obtained future climate timeseries from both RCP 4.5 and RCP 8.5 climate scenarios, where RCP 4.5 scenario represents a decline in greenhouse emissions around year 2040 and RCP 8.5 is a "business-as-usual" scenario with a continuous rise in greenhouse emissions. Both scenarios predict a global rise in temperature.

Choosing temperature and precipitation data of the single GCM grid point containing ICB, we used quantile delta mapping (QDM) ("MBC" package in R) to bias correct the GCM data and downscale it to the location of the Yosemite Headquarters weather station. QDM is a non-parametric method to correct systematic modeled biases with respect to observed values while preserving model-projected relative changes in precipitation and temperature quantiles (Cannon et al., 2015). In addition to modeled, observed, and future climate timeseries, QDM requires observed climate observations, which we obtained from the Yosemite Headquarters weather station and gap filled via multivariate imputation ('MICE' package in R) and data from adjacent weather stations (see Appendix Section B). We bias-corrected the daily precipitation and the daily maximum and minimum temperatures for 2030–2070, treating the historical period (1970–2010) as static. During a static period, the distribution of climatic variables does not change significantly for any decade. QDM was then used to superimpose the modeled quantile trends ("delta changes") onto the observed static period. The delta changes were applied multiplicatively to the precipitation correction and additively to the temperature corrections (Cannon et al., 2015). The resulting bias-corrected model timeseries form the climate ensemble were used to drive RHESSys modeling. The timeseries were summarized in terms of rainfall, temperature, snowfall, and snow season statistics across the ensemble: these quantities are important determinants of the length of the fire season and basin hydrology.

Although CO_2 concentrations are predicted to rise in the future climate, due to model limitations, they are held constant across all model simulations.

2.6. Model experiments

The model experiments were set up to answer the Research Questions. Prior to conducting the model experiments, RHESSys was initialized with the 1969 fire-excluded vegetation map, which was spun-up for a few hundred years using observed historical climate (repeated time-series), starting from no carbon stores, and until LAI reached a steady-state (Boisramé et al., 2019). Then, prior to the future climate simulations (2030–2070), for each RCP scenario, the 1969 fire-excluded and spun-up vegetation was further spun-up using the 2020–2030 climate.

Research Question (i) asks how changing climate would alter the hydrology of the fire-excluded ICB, assuming vegetation was initialized in the same state as was observed in 1969. To answer this question, we held vegetation type constant and ran RHESSys for 40 years using the observed 1970–2010 climate, and for the RCP 4.5 and 8.5 future 2030–2070 climates (see Fig. 4). Differences in the predictions can be interpreted as the impact of climate on vegetation and hydrology in the absence of changes imposed by fire.

Research Question (ii) addresses the differences in how wildland fire use affects ICB hydrology under future versus observed climates. To answer this question we ran RHESSys for a 40 year period using the observed 1970–2010 climate, and for the future climate ensemble for the period 2030–2070 under RCP 4.5 and RCP 8.5 scenarios.

For each of these climates we ran a control model representing fire excluded conditions based on the 1969 vegetation map (Fig. 2-A) with no fire disturbance imposed ("fire excluded"). We also ran a treatment model in which fire disturbance was imposed based on the observed historical (1970–2010) fire regime ("historical frequency") and updated vegetation maps after fires (using both the observed post-fire vegetation transitions and the bounding cases where all vegetation transitions to specific cover types). The differences in hydrological predictions between control and treatment models can be attributed to the effects of fire on vegetation and litter. The differences in these differences (sensu Angrist and Pischke, 2008) can be attributed to the role of different climates interacting with the fires.

Research Question (iii) is addressed by repeating this analysis using the higher frequency fire regimes in combination with the future climate scenarios (Fig. 4), however, in this case, only historical vegetation transitions were modeled. Again, the fire excluded landscape was modeled across all climate regimes as a control. Differences between control and treatment can again be attributed to the role of fire.

RHESSys output was generated on daily timescales at the scale of the entire Illilouette Creek Basin. The analysis focuses on streamflow, vertically aggregated depth of saturated and unsaturated groundwater storage ("subsurface storage"), snow water equivalent (SWE), snow sublimation, LAI, evaporation, and transpiration. These variables were aggregated to water year to visualise long-term fire effects. All results were reported as a depth of water, with basin-scale fluxes normalized by the basin area (150 km^2). However, in interpreting these results, it is important to recall that all changes in basin-scale hydrology were derived from fire-induced changes that occurred in at most 75% (112 km^2) of the watershed. If considering how the observed changes in ICB might play out in other watersheds, it may be more appropriate to weigh these changes by fire-affected area in each basin. Heterogeneity in hydrological processes should also be considered: for example, only approximately 52% of the streamflow in ICB is generated in the area that burned (and the remaining 48% is generated on high elevation rock and

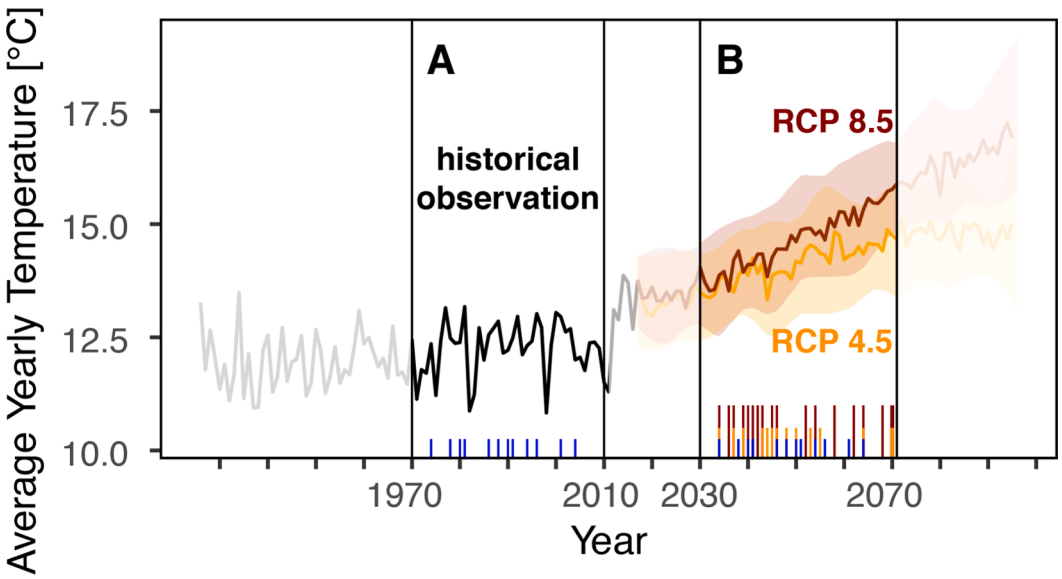

Fig. 4. Historical modeling time period from 1970 to 2010 (A), denoting observed 40 years since the end of fire exclusion policies in the ICB. Future modeling time period from 2030 to 2070 (B) is compared to the historical one. An ensemble of 10 different CMIP5 general circulation models (GCMs) was used as future climate inputs for two different representative concentration scenarios (RCP 4.5 and RCP 8.5). Blue vertical lines denote historical frequency fire events. Orange vertical lines deNote 30% increase in fire frequency from historical observations, and dark red vertical lines deNote 60% increase in fire frequency.

is largely uninfluenced by downgradient vegetation condition). Snowpack dynamics are also highly spatially variable, with these spatial patterns shifting greatly between climate scenarios. These variations are masked in the whole-of-basin averaging used to present hydrological change in this study, but analysis of heterogeneity in hydrological response to fire is beyond the scope of this manuscript.

2.7. Uncertainty analysis

Recognizing that the scenarios modeled do not fully bound the range of possible fire-climate-vegetation interactions, our uncertainty analysis follows the GLUE approach to constrain the combination of uncertainty due to climate projections and hydrological parameter uncertainty. Each hydrological model experiment consisted of running the 93 highest performing calibration parameter ensembles, in conjunction with the 10 climate model ensemble members. Thus each combination of a future climate scenario (RCP 4.5 or RCP 8.5) and a fire scenario (exclusion, observed historical, +30%, or +60%) generated an ensemble of 930 modeled timeseries for each variable (93 RHESSys model parameterizations times 10 climate models). This ensemble formed the basis for uncertainty analyses. In general, the question we were asking was related to the significance (relative to parameter and climate model uncertainty) of differences in predicted values of any hydrological variable between two scenarios. To compute this significance, we differenced model output from equivalent ensemble members (having the same combination of driving climate model and RHESSys model parameters) from the two scenarios of interest. This generated a set of 930 differences (except in the case where fire scenarios were compared for the observed climate, when 93 differences result). The 95% confidence interval was then specified as the interval between the 2.5 and 97.5 percentiles for these 930 differences. If this interval excluded zero, the difference was considered significant at the 95% confidence level. See Appendix D for a mathematical formulation of how the ensemble of differences was calculated.

3. Results

3.1. Future climate

Table 1 shows climate statistics aggregated by decade for the 4 decades of simulation, where decades 1, 2, 3, and 4 correspond to the historical time periods of 1971–1980, 1981–1990, 1991–2000, 2001–2010, and future time periods of 2031–2040, 2041–2050, 2051–2060, 2061–2070 respectively. By considering output on this decadal basis, we can better compare between climates based on the common time since first fire (first fire occurs in 1974 for the historical modeling and 2034 for future model scenarios). Each decadal value shown is based on the average of the 10 GCM models following downscaling and bias correction. All results discussed below refer to comparisons between 1970–2010 historical averages, and 2030–2070 future climate simulations. By 2060–2070, ICB will warm by 2.2 °C under RCP 4.5 and by 3.1 °C under RCP 8.5 climate scenarios. Predicted annual precipitation totals in both scenarios are slightly wetter than the historically observed record. The 2030–2070 RCP 4.5 climate, on average, receives 159 mm more precipitation per year than the 1970–2010 period, while RCP 8.5 receives 32 mm more. The historically observed precipitation lies within the 95% uncertainty bounds of both future climate ensembles, meaning that some models predict a drier and others a wetter future climate. Ensemble-averaged precipitation under both RCP 4.5 and 8.5 scenarios exhibits much less inter-annual variability than do historical observations (see Appendix Fig. B.3-A), which is a result of averaging over the ensemble. The RCP 8.5 climate ensemble distributions of daily precipitation show an increase in extreme events when compared to the historically observed precipitation distribution (see Appendix Fig. B.4). Higher average temperatures, with similar total precipitation, result in a shorter snow season. On average, by 2060–2070, the snow season length drops by 26 days for RCP 4.5 and 43 days for RCP 8.5 climates. Additionally, and again due to the warmer temperatures, the snow fraction of precipitation (% precipitation falling as snow) declines for future climates. Historically, 60–70% of precipitation in ICB occurred as snowfall, and this percentage falls to 49% (RCP 4.5) and 42% (RCP 8.5) by 2060–2070.

Table 1
Bias-corrected yearly average temperature data and precipitation yearly sums are averaged decadaly and presented as an average of all 10 GCM models for both RCP 4.5 and RCP 8.5 scenarios. Decades 1, 2, 3, and 4 refer to the historical time periods of 1971–1980, 1981–1990, 1991–2000, 2001–2010, and future time periods of 2031–2040, 2041–2050, 2051–2060, 2061–2070 respectively. Temperature and precipitation data were used as RHESSys model inputs while maximum snow depth, snow season length, and % of precipitation as snow are based on RHESSys fire excluded model outputs. Gray shading indicates that the variable in the future climate scenario is statistically different from the observed climate scenario at the 95% confidence level.

	Decade			
Climate	1	2	3	4
	Temperature [°C]			
Observed	12.0	12.3	12.4	12.3
RCP 4.5	13.7	14.0	14.4	14.5
RCP 8.5	14.0	14.3	14.9	15.4
	Precipitation [mm]			
Observed	929	937	1071	745
RCP 4.5	1125	1026	1059	1106
RCP 8.5	914	987	976	933
	Snow Season Length [days]			
Observed	213	213	212	208
RCP 4.5	182	174	173	176
RCP 8.5	180	180	171	158
	% Precipitation as Snow			
Observed	66	63	67	70
RCP 4.5	54	54	48	48
RCP 8.5	54	49	45	42

3.2. Hydrological outcomes of wildfires

To understand the hydrological outcomes of wildfire, we considered multiple hydrological variables at the annual scale (transpiration, evaporation, streamflow, subsurface storage, and maximum snow water equivalent) and their mean values across all model parameter sets and climate ensemble members. We averaged the value of these variables on decadal timescales, and Table 2 shows these decadal averages for the observed, RCP 4.5, and RCP 8.5 climate scenarios for the four fire regimes: fire excluded, historical fire frequency, and +30% and +60% fire frequency. The analysis of the results is broken down based on the model scenarios, showing the changes in hydrology due to: 1) climate only, 2) climate in combination with the historical wildland fire use regime, and 3) climate combined with hypothetical, higher-frequency fire regimes.

3.2.1. Climate only

Answering Research Question (i) isolates the influence of climate on hydrology if vegetation was to remain in a fire-excluded state. Overall, other than expected but statistically non-significant decreases in

Table 2
Hydrological variables averaged decadally for all climate and fire scenarios. Decades 1, 2, 3, and 4 refer to the time periods 1971–1980, 1981–1990, 1991–2000, and 2001–2010 for the observed climate, while for future climate scenarios (RCP 4.5 and 8.5) these decades refer to 2031–2040, 2041–2050, 2051–2060, and 2060–2070 respectively. Grey highlighting indicates a significant difference between modeled variables in the future climate and the historically observed climate (Using Eq. D.2). An asterisk indicates that wildfires significantly affected the modeled hydrological variable (Using Eq. D.1). Change is reported as significant if the 95% confidence interval for the difference between two fire-climate model scenarios does not include zero.

Scenario		Decade			
Fire	Climate	1	2	3	4
		Transpiration [mm/year]			
Fire Excluded	Observed	59	60	65	53
	RCP 4.5	71	67	70	72
	RCP 8.5	60	62	63	63
Historical Frequency	Observed	58*	57*	59*	41*
	RCP 4.5	70	65	64*	57*
	RCP 8.5	59*	59	56*	48*
+30%	RCP 4.5	70	62*	57*	54*
	RCP 8.5	59	56*	49*	45*
+60%	RCP 4.5	69*	56*	54*	54*
	RCP 8.5	59*	50*	45*	45*
		Evaporation [mm/year]			
Fire Excluded	Observed	88	79	76	81
	RCP 4.5	89	89	87	89
	RCP 8.5	70	68	66	63
Historical Frequency	Observed	87*	78*	74*	75*
	RCP 4.5	89*	88*	84*	80*
	RCP 8.5	69*	67*	64*	57*
+30%	RCP 4.5	89*	86*	79*	78*
	RCP 8.5	69*	66*	60*	56*

(continued on next page)

Table 2 (*continued*)

Scenario		Decade			
Fire	Climate	1	2	3	4
+60%	RCP 4.5	88*	82*	78*	79*
	RCP 8.5	69*	64*	59*	56*
		Streamflow [mm/year]			
Fire Excluded	Observed	957	974	1133	752
	RCP 4.5	1162	1072	1111	1181
	RCP 8.5	963	1012	1024	991
Historical Frequency	Observed	957	977	1141	769
	RCP 4.5	1164	1075	1120	1204
	RCP 8.5	964	1016	1033	1010
+30%	RCP 4.5	1164	1080	1130	1210*
	RCP 8.5	964	1020	1042	1016
+60%	RCP 4.5	1164	1088	1136*	1209*
	RCP 8.5	964	1027	1048*	1015
		Subsurface Storage [mm]			
Fire Excluded	Observed	1711	1708	1700	1707
	RCP 4.5	1701	1700	1700	1694
	RCP 8.5	1708	1705	1706	1705
Historical Frequency	Observed	1712	1714	1713*	1740*
	RCP 4.5	1702	1707	1716*	1730*
	RCP 8.5	1709	1712	1722*	1740*
+30%	RCP 4.5	1702	1712	1732*	1737*
	RCP 8.5	1709	1717*	1737*	1746*
+60%	RCP 4.5	1703	1726*	1742*	1738*
	RCP 8.5	1710	1730*	1747*	1748*
		Max Snow Water Equivalent [mm]			
Fire Excluded	Observed	600.1	572.9	743.5	513.6
	RCP 4.5	569.3	523.9	463	471.8
	RCP 8.5	491.1	458.3	415.4	367.8
Historical Frequency	Observed	600.2*	573.4*	744.4*	517.1*
	RCP 4.5	569.4	524.3	463.8	475.0*
	RCP 8.5	491.2	458.6	416.1	369.7*

Scenario		Decade			
Fire	Climate	1	2	3	4
+30%	RCP 4.5	569.5	525.2*	465.6	475.9*
	RCP 8.5	491.2	459.3	417.4*	370.0
+60%	RCP 4.5	569.6	526.4	466.2*	475.3*
	RCP 8.5	491.2	460.0	418.0*	370.1

*: Difference between burned and fire excluded scenarios is statistically significant at 5% level.
Grey Shading: Future fire-climate scenario is statistically different from observed fire-climate scenario at 5% level.

snowpack, the different climate scenarios cause only minimal changes in predicted ICB hydrology at annual timescales. To discuss these changes we focus on the final decade of simulation (i.e. 2000–2010 and 2060–2070). Trends in all water balance components across the climate scenarios are shown in Fig. 5-A as a fraction of annual precipitation. Streamflow is always the largest component of the water balance, representing 83.4% (observed), 86.1% (RCP 4.5) and 86.7% (RCP 8.5) of precipitation. Independent of the climate scenario, transpiration represents 6% of annual precipitation, meaning it increased in absolute terms in the slightly wetter climate projections (by 19 mm for RCP 4.5 and 10 mm for RCP 8.5). The small projected increases in streamflow as a fraction of the water balance in RCP 4.5 and 8.5 can be attributed to reduced evaporation (litter, canopy, and soil evaporation, excluding transpiration, plus snow sublimation), which declines from 10.4% of precipitation (observed climate) to 7.7% (RCP 4.5), and 6.8% (RCP 8.5), almost entirely due to lower snowpack - and thus sublimation - in the warmer climates. Unsurprisingly, the maximum basin-averaged snow water equivalent decreases in future climates, by 42 mm (RCP 4.5) and 146 mm (RCP 8.5) relative to observed climate conditions ("Fire Excluded" in Table 2). Lower snowfall and snowpack also reduce the fraction of streamflow derived from snowmelt and move the month of peak streamflow earlier. For example, peak snowmelt occurs in May for 2000–2010, but in April for 2060–2070, in both RCP 4.5 and RCP 8.5 scenarios. In this peak snowmelt month, the proportion of streamflow derived from snowmelt declines from a historical maximum of 95% (2000–2010), to 83% and 79% (2060–2070, RCP 4.5 and RCP 8.5 respectively, see Appendix Fig. E.3-A and B). Notably, in this final decade there are no observed trends in subsurface storage (ΔS in Fig. 5-A, where ΔS is the net change in storage over one water year, is near zero). This means that the differences in water balance across the climate scenarios are exogenously driven, rather than arising from non-stationarity associated with interannual trends of wetting or drying of the basin.

Lastly, the only significant changes in future climate when compared to the observed climate (gray shading in Table 2) is a 19 mm/year increase in transpiration (RCP 4.5 climate) and a 18 mm/year decrease in evaporation (RCP 8.5). This lack of significance is associated with high uncertainty of both climate models and hydrological parameters which is a common phenomenon in hydrological models (Her et al., 2019; Najafi et al., 2011). Even if they are not statistically significant, there are clear trends in hydrological variables across climate scenarios; particularly there is higher transpiration, increased streamflow, and decreased maximum snow water equivalent for RCP 4.5 and 8.5 climate scenarios compared to the historical baseline (Table 2).

3.2.2. *Climate + historical fire regime*

This section addresses Research Question (ii), which asks how the hydrological outcomes of fire use strategies in ICB would differ under future climate conditions (2030–2070, RCP 4.5 and RCP 8.5), relative to those outcomes under the observed climate (1970–2010). Answering this question repeats the analysis above, but including fire under the "historical frequency" model scenario, enabling us to compare the differences in hydrology associated with fire between different climate scenarios. These model runs were conducted for both the observed post-fire vegetation succession and for bounding cases where all post-fire vegetation in high severity burn areas was forced to transition to a single vegetation type. These "bounding" cases suggest that the hydrological changes predicted have low sensitivity to the type of vegetation regrowing in high severity burn areas (Fig. 2). Subsurface storage and streamflow were almost entirely insensitive to the vegetation transitions prescribed, regardless of the future climate scenario, and variations in

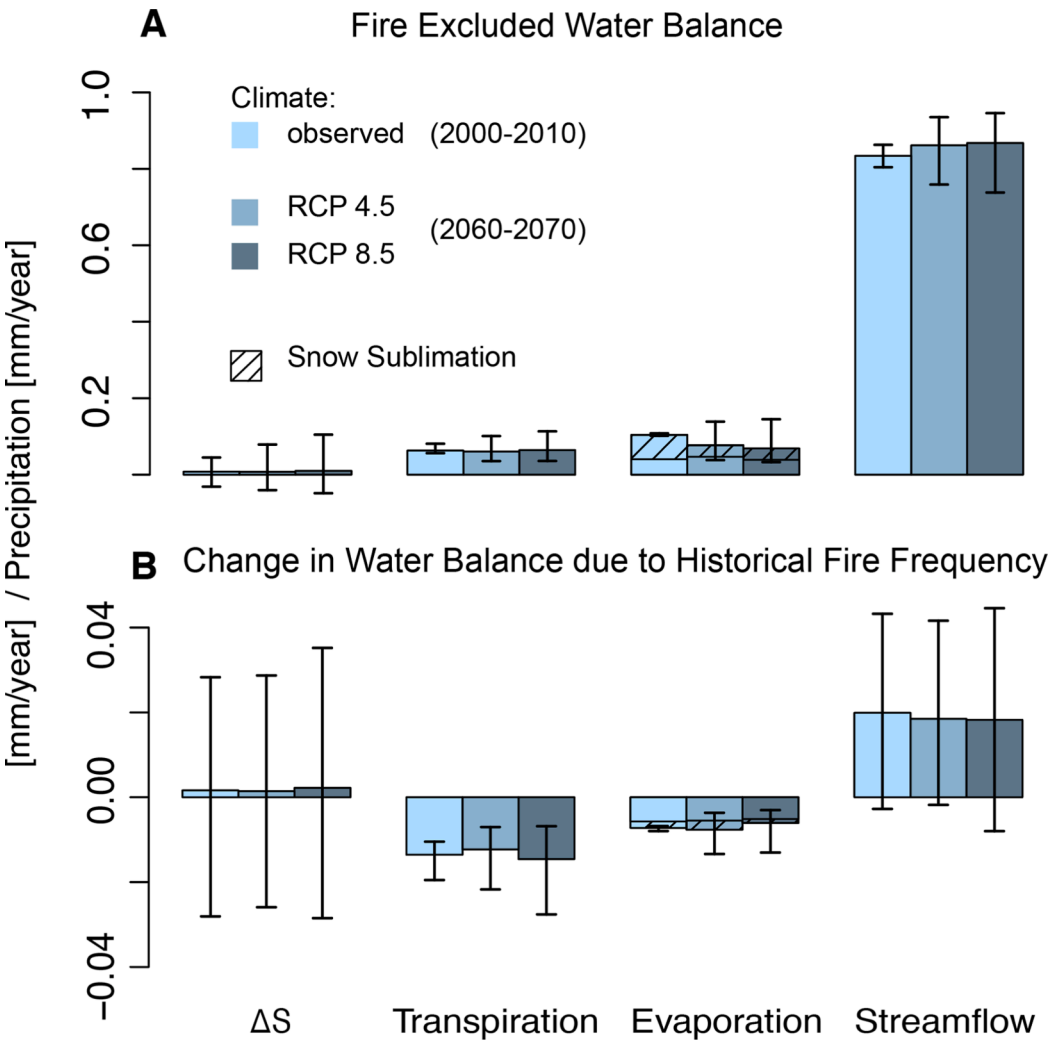

Fig. 5. A: Water balance for the fire-excluded scenario. Subsurface storage change (ΔS; the change in subsurface water storage from one water year to the next), transpiration, evaporation, and streamflow are normalized to precipitation. B: Modeled average change in water balance variables due to fires normalized to precipitation. In both A and B, results are shown for the final simulated decade (resulting in most change). Historically observed fire frequency scenario is used for the difference in B. Error bars represent 95% confidence interval across all climate scenarios, parameter sets, and years within the final simulated decade.

the predicted change in other hydrological variables across vegetation types were on the order of < 10%, being largest where vegetation was forced to regenerate as conifers. A more detailed analysis of the uncertainty due to the prescribed successional trajectories is provided in Appendix F, but considering this limited sensitivity, we focus here on the models using the observed vegetation transitions only.

Detailed results, showing water balance components for each scenario, are provided in Table 2. Timeseries results showing how the historical fire regime influenced the trajectory of hydrological variables in the different climates are shown in the first column of Fig. 6. Again we focus the discussion here on the final simulated decade and discuss the magnitude of the differences in the fire-induced changes that arise in the different components of the water balance across the climate scenarios for this decade.

Similarly to the fire-excluded condition described in Section 3.2.1, there are few statistically significant differences between future climate conditions and observed climate under a historical fire regime; comparing future climate of 2060–2070 to observed climate of 2000–2010, the only statistically significant differences (gray shading in "Historical Frequency" rows in Table 2) were observed for RCP 4.5 transpiration (16 mm/year greater than observed climate) and RCP 8.5 evaporation (18 mm/year decrease). In this paragraph we compare ICB's hydrology under historical fire frequency to ICB's hydrology under fire excluded conditions. Though there is little significant difference across climate regimes in a basin experiencing historical fire frequency, many changes induced by fire – compared to a fire excluded scenario – are significant (asterisks in Table 2). For RCP 4.5, by the final decade of simulation, statistically significant declines in transpiration (15 mm/year) and evaporation (9 mm/year) are associated with a statistically significant increase in subsurface water storage (34 mm/year), a statistically-significant but small increase in peak snow water equivalent (3.2 mm/year), and a non-significant 23 mm/year increase in streamflow. For RCP 8.5, historical frequency fire regime results in statistically significant decreases in transpiration (15 mm/year) and evaporation (6 mm/year), increases in subsurface water storage (35 mm/year) and peak snow water equivalent (2.9 mm/year), and a non-significant increase in streamflow (19 mm/year). The results do suggest that fire management could slow the climatically driven loss of snowpack in the ICB; although climate warming reduces snowpack, there is more snowpack in a given future climate in the context of wildfire compared to fire exclusion (Table 2).

The overall effect of the historical frequency fire regime across all climates is to decrease the relative importance of transpiration and evaporation, where transpiration declines by 1.4%, 1.2%, and 1.5% and evaporation declines by 0.7%, 0.8%, and 0.6% for observed, RCP 4.5, and RCP 8.5 climates respectively (Fig. 5-B). The decline in precipitation-normalized evaporation and transpiration results in an increase of the runoff ratio by 1.91%, 1.85%, and 1.82% for observed, RCP 4.5, and RCP 8.5 climates respectively. Fire-induced change in annual soil storage gain/loss is <1% across all climates.

Other indicators of hydrological function in the basin are also similar across the climate scenarios – for example, most streamflow increases

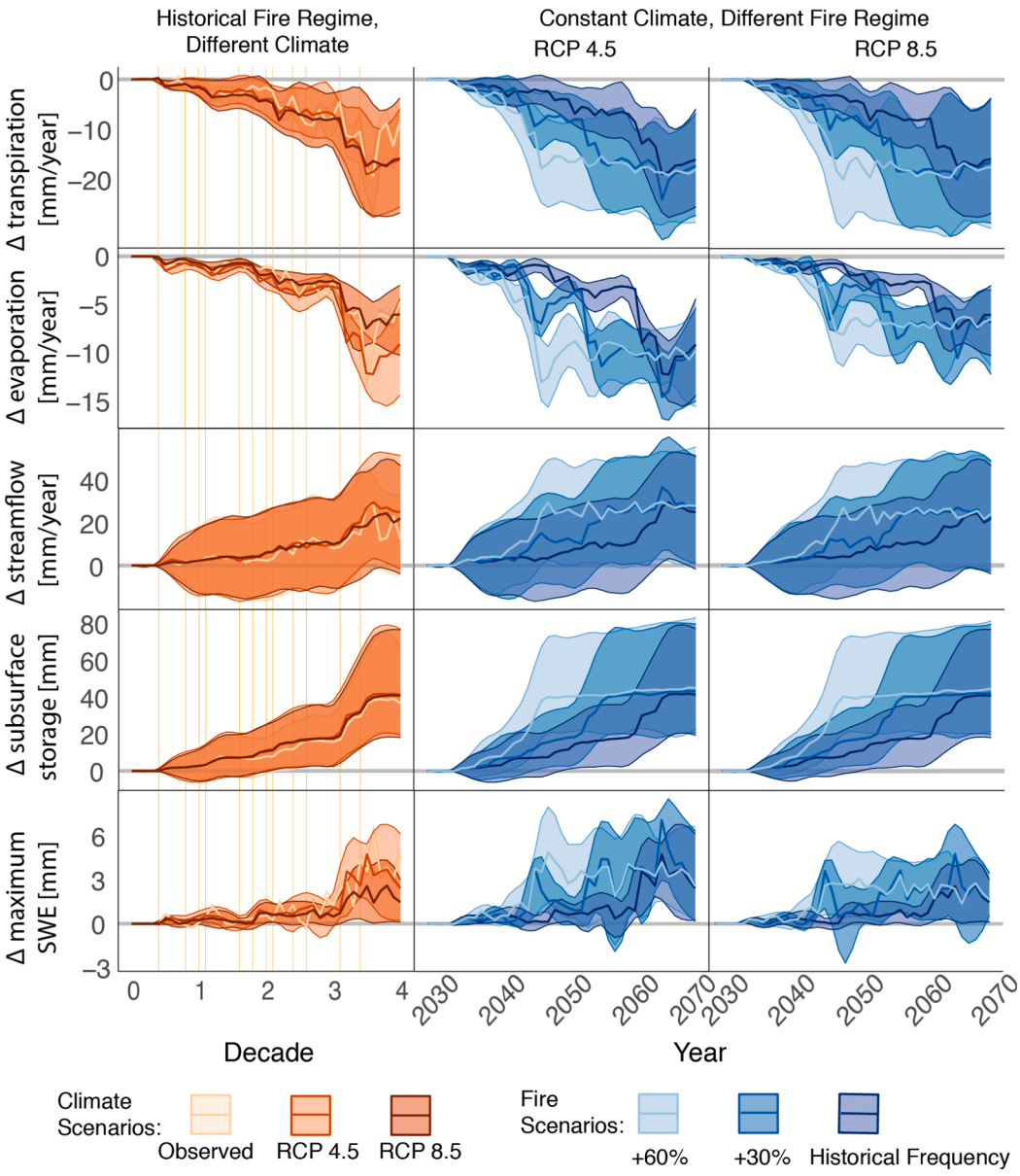

Fig. 6. All plots show the difference between the burned and fire excluded ICB. Plots in blue have constant climate (RCP 4.5 in left panel and RCP 8.5 in middle panel), but vary the fire frequency scenario. Plots in red keep the fire frequency constant (historical), but vary the climate scenario. Vertical orange lines in the right panel indicate a historical fire occurrence. Shading indicates 95% confidence interval of the 93 observed climate or 930 future climate model runs (93 parameter sets for each of the 10 GCMs or 1 observed climate), while thick lines represent average difference. Vertical axis has the same scale for each hydrological variable. Decade 0, 1, 2, 3, and 4 refer to years 1970, 1980, 1990, 2000, and 2010 for observed climate and years 2030, 2040, 2050, 2060, and 2070 for RCP 4.5 and RCP 8.5 climates. (For interpretation of the references to color in this figure legend, the reader is referred to the web version of this article.)

due to fire occur during peak snowmelt, regardless of climate scenario (see Appendix Fig. E.3). The increases in peak snow water equivalent due to the imposition of fire use are caused by decreases in sublimation and canopy interception (see Appendix Figs. E.4 and E.1), again mostly independently of the climate scenario. Fire use causes snowmelt to become less important as a driver of streamflow; snowmelt explains at most 38%, 47%, and 31% of the fire-induced change in streamflow for observed, RCP 4.5, and RCP 8.5 climates, respectively, by 2060–2070 (see Appendix Fig. E.3-D,E,F).

The impacts of fire use policies on hydrology are more apparent amongst climate scenarios when considering intra-annual responses. Under the observed climate, wildfire use causes the greatest change to streamflow (relative to fire exclusion) during the peak snowmelt months of March through May. However, wildfire use under future climates significantly increases streamflow relative to fire excluded conditions for the period of October through May (for the final decade of simulation). Little change in streamflow is modeled during the summer months (June-September) in any fire/climate scenario (Appendix Fig. E.3-D,E,F). The maximum change in transpiration due to fire occurs one month earlier (June) under the RCP 4.5 and RCP 8.5 climate scenarios than it does under observed climate (see Appendix Fig. E.2).

Overall, these results suggest that the changes associated with fire use in the ICB during the 1970–2010 period are highly comparable to those that would be predicted if the same set of fires and vegetation changes occurred under future climate conditions. This is visually evident in the right-hand column of Fig. 6, where trajectories of hydrological change and its confidence interval under different climate scenarios track each other closely for most variables.

3.2.3. *Climate + changing fire regimes*

Research Question (iii) asks how sensitive the hydrological outcomes of fire use strategies for the 2030–2070 period were to potential increases in fire frequency. Again, we focus on the results for the observed vegetation transitions only. Detailed results, showing water balance components for each scenario, are provided in Table 2. Different fire regimes influence the trajectory of hydrological variables in the different climates as shown in the left hand columns of Fig. 6. These plots show that the most dramatic effect of the increasing fire frequency is to reduce the time needed to approach a pseudo-steady condition, which itself is very similar across the climate scenarios. Since the first wildfire

occurrence, it takes approximately 13, 22, and 30 years to observe maximum changes in most water balance components under the +60%, +30%, and historical fire frequency scenarios respectively. These distinctions in timing are most easily observed in the subsurface storage and streamflow plots of Fig. 6. Increasing fire frequency increases the maximum observed changes slightly in the hydrological variables, where +60% fire frequency scenario generally results in greatest hydrological change across climate scenarios.

With the exception of streamflow, all water balance variables experience significant change due to fire, across all climate and fire regimes, by the final simulated decade. Streamflow increases relative to fire excluded conditions under all scenarios, although the increases are significant only for certain climate and fire scenarios: for the RCP 4.5 climate scenario streamflow is significantly higher in the final simulated decade of the +30% fire frequency scenario and the last two decades of the +60% fire frequency scenario, and in the RCP 8.5 climate scenario streamflow increase is only significant in the third decade (2050–2060) of the +60% fire frequency scenario. The decades with significant increases in streamflow due to fire correspond to decades with greater precipitation and decades in which many fire events occur. Averaging across the final simulated decade, the greatest changes between fire scenarios compared to the fire excluded scenario for the same climate are: an 18 mm decrease in transpiration (RCP 4.5, +30%), and 11 mm decrease in evaporation (RCP 4.5, +30%), a 29 mm increase in streamflow (RCP 4.5, +30%), a 44 mm increase in subsurface storage (RCP 4.5, +60%), and a 4.1 mm increase in maximum snow water equivalent (RCP 4.5, +30%). With the exception of maximum snowpack, the historical fire regime always produced the smallest changes in hydrological variables for each climate type (Fig. 2). The different pace of change across the scenarios is closely related to the rate of change of LAI: more frequent fires cause a more rapid decline in LAI (see Appendix Fig. E.1). In the final simulated decade, LAI had declined by 0.07 and 0.08 for RCP 8.5 and 4.5 climate scenarios respectively (historical fire regime), by 0.10 and 0.11 (30% increase), and 0.08 and 0.09 (+60%), relative to the fire excluded cases (see Appendix Table E.1).

One possible risk associated with fire use strategies is that by removing vegetation from the ICB, the peak flow and flood risks might increase. Noting that the model calibration was not optimized to predict peak flows (Boisramé et al., 2019), we nonetheless examined the largest daily streamflows for each year, and how these varied with fire regime and climate forcing. The maximum daily flow increased by about 3.2% due to fire in the final simulated decade – an increase that did not vary across the different climate and wildfire scenarios, and which was not statistically significant relative to model uncertainty (see Appendix Fig. E.5).

4. Discussion

4.1. Impacts of fire use on ICB hydrology under future climates

The modeling efforts presented here suggest that fire use strategies will have a similar impact on the hydrology of the ICB under future climates to that which occurred due to the historical fire management from 1972 - present - namely modest increases in streamflow, driven primarily by reductions in vapor fluxes, particularly sublimation and evaporation (see Boisramé et al. (2019) for additional detail on fire-induced decreases in evaporation), and increased subsurface water storage. The broad similarity in these outcomes is perhaps unsurprising given the modest changes in water balance predicted for fixed, fire-suppressed, vegetation cover when climate change alone is considered. These differences may be increased in models that are able to consider variation in CO_2 concentration across the future climate scenarios, unlike the present model which held CO_2 constant in all scenarios.

Initiating a fire use strategy in 2030 is predicted to increase streamflow by an average of 19–29 mm/year by 2070, relative to maintaining fire exclusion (c.f. a 17 mm/year historical increase). Although the predicted streamflow increases are not always statistically significant given the uncertainties associated with future climate and the hydrological model parameters, the drivers of this increase - greater snowpack and subsurface storage and reductions in evaporation and transpiration due to fire use relative to fire suppressed conditions, are significant in all climate and fire frequency scenarios. Future applications of fire use strategies in the ICB would therefore be likely to increase natural water storage in the basin, and may result in increased streamflow. Increasing fire frequency, while maintaining similar spatial fire severity distributions to the historical period, has the primary effect of speeding up the rate of change, without altering the final hydrological state of the basin greatly. The final hydrological state predicted for the ICB was largely robust to changes in the post-fire vegetation transitions used in the model; model scenarios in which highly burned regions transitioned to coniferous forests, shrublands or wetlands diverged minimally from each other.

We did not quantitatively explore the robustness of these final states to our modeling decision to use historical fire areas and severities to represent these elements of future climate, but the consequences of these decisions can be qualitatively explored. For example, the similarity in the final hydrological state of the basin across fire frequency scenarios may be partly attributable to the re-use of the same fire perimeters in all scenarios – all cases converged on a similar basin-averaged LAI independently of the fire frequency. These fire perimeters do, however, cover 75% of the vegetated area of ICB, so that the modeled fires affected most of the area of the ICB that can burn. However, by preventing fire from burning into areas that did not experience a fire in 1970–2010, the modeled fire perimeters may under-estimate the maximum vegetation changes which could be induced in ICB, thus also underestimating the extremes of vegetation and hydrological changes that could be induced by fire. On the other hand, a scenario where the historical perimeters over-estimate fire extent and severity seems probable due to additional fuel reductions. Consideration of this fuel limitation means the use of historical fire severity in the models is likely an upper bound on future fire severity. Therefore, it is likely that uncertainties in the future fire regime associated with our fire modeling choices are opposite in sign and likely to mitigate each other.

Our work has focused on representing known fire impacts of a frequently-burned watershed rather than modeling them and thus introducing additional uncertainty. However, there is promising work being done coupling RHESSys to a fire spread model (WMFire) which uses RHESSys fuel loads and water deficits to model fire spread for a given location (Kennedy et al., 2017; Bart et al., 2020). Both studies have demonstrated that such coupling can re-produce realistic historical fire regime characteristics across different eco-systems and stand-ages without being specifically tuned to do so. Further validation of this coupled model is needed, especially its representation of the sensitivity of fire-vegetation feedbacks to a changing climate. Future work will explore the potential of RHESSys-WMFire to study fire-hydrology-vegetation feedbacks in ICB.

While the eco–hydrological model used in this study has been successfully validated using a number of streamflow metrics, it was not configured to capture high flow events (important for flood and erosion management) due to the lack of high-resolution precipitation and streamflow observations. The model also ignores post-fire changes to soil properties which could lead to greater overland and streamflow from heightened soil water repellency. Within these limitations, modeling suggests that fire use in the ICB would increase peak streamflow by at most 3.2% from fire excluded conditions for all climate and fire regime scenarios. This increase is likely under-predicted.

In spite of the limitations on the modeling, which mean that results should not be interpreted as a forecast of absolute hydrological behavior in fire-affected watersheds like the ICB, it is important to recognise that the limitations also affect the historical baseline estimates of hydrological change from 1970–2010 similarly to future modeled scenarios.

Thus, we can conclude that fire use policies implemented in fire-suppressed basins similar to ICB and generating similar or more frequent fire regimes, would generate similar hydrological co-benefits to those experienced to date.

4.2. Management implications

These hydrological co-benefits may be an essential component of building an economic case for forest management, because the economic investment needed to implement forest management strategies remains an impediment to their uptake (González-Sanchis et al., 2019). For instance, although the streamflow gains predicted from ICB to date are modest on a per-area basis in the watershed, the additional streamflow gains from ICB alone could produce $1.5–2.3 million of hydropower revenue per year, and represent a volume equivalent to approximately 5.1% of the city of San Francisco's annual water use, which itself is worth approximately $6.0–9.2 million in water sales from the San Francisco Public Utility Commission (detailed calculations in Appendix-G). Although the ICB does not directly feed the Hetch Hetchy reservoir that forms San Francisco's water supply, these figures provide an indication of the potential economic value of even modest local changes in water balance, which could be driven by fire use policies. Of course, this value would be offset by the costs of the negative impacts of wildfire on watersheds, such as increased erosion and declines in water quality (Tiedemann et al., 1979; Smith et al., 2011), which should also form part of any economic analysis of wildfire use policies. To date, there is no evidence of extensive erosion or downstream water quality declines in response to ICB wildfires, but work to better establish the potential scope of such problems remains needed.

The ICB remains a unique long term experiment on the effects of fire restoration on forests and water balance, but policy is shifting to extend fire restoration across the Sierra Nevada. For example, current revisions to the Land and Resource Management Plans for National Forests (NF) in the southern Sierra Nevada emphasize fire use for resource benefit over some 69 to 84% of National Forest land. Boisramé et al. (2017a) estimated that approximately 19,100 km^2 of the Sierra Nevada region is topographically and climatically similar to ICB, and may be suitable for similar fire use strategies. However, to achieve similar hydrological outcomes as in ICB, fire use in other basins would also need to achieve the substantial changes in forest cover that occurred in that Basin. In the only other basin in the Sierra Nevada with a multi-decadal history of fire use policies, Sugarloaf Creek Basin in Sequoia-Kings Canyon National Park, greater fire suppression activity in the recent decades and lower productivity forests have led to a much more modest impact of fire on vegetation than observed in ICB (Stevens et al., 2020). The relatively limited sensitivity of predicted hydrological outcomes to climate, however, suggests that extension of the fire use policy beyond ICB to other productive and topographically suitable forests could produce modest but valuable increases in streamflow.

5. Conclusion

Downscaling and bias correction of climate projections for ICB and their use in the RHESSys hydrological model suggest that the modest increases in streamflow estimated to have occurred due to fire use policies in the late 20th – early 21st Century are likely to be robust to the warmer future climate. Although the timing and provenance of streamflow shifts earlier in the year and towards rainfall rather than snowmelt, these changes are not projected to result in large alterations in annual water balance partitioning. To summarize our response to the posed questions:

i) In the absence of fire use policy, hydrology of the ICB is relatively similar during RCP 4.5 and RCP 8.5 2030–2070 climates and under the observed historical climate of 1970–2010 (in terms of annual volumes of various fluxes). One notable difference is the reduction of snowpack which leads to lower total evaporation (due to a reduction in sublimation) in the future climate scenarios.

ii) The hydrological outcomes of fire use strategies in ICB under future climate conditions are similar to those under observed climate. The historical fire frequency regime produces similar reductions in evaporation and transpiration and gains in streamflow across all climates. Fire-induced increase in snowpack partially counteracts climate change induced reductions in snowpack.

iii) Considering fuel-limited conditions in ICB, anticipated increases in fire frequency (due to ignitions and not fuel availability) in the future climate of 2030–2070 will lead to similar hydrologic changes as historic fires, but in a shorter timeframe.

Though we provide a broad range of possible fire regime outcomes, future work should focus on fully coupling post-fire vegetation transitions to climate and hydrology and consequent fire-regime. More advanced modeling of fire effects on hydrology may be needed as well; in addition to wildfire impacts on vegetation removal, changes to soil properties are needed to accurately model high intensity precipitation events that have an impact on erosion, flooding, and water quality.

Rising temperatures and a naturally volatile hydroclimatic setting present ongoing challenges to California's water supply security and forest resilience. This study suggests that where self-limiting fire behavior, as per ICB, can be anticipated, the hydrological co-benefits should be considered as part of future fire policy development and cost-benefit analysis.

CRediT authorship contribution statement

Ekaterina Rakhmatulina: Investigation, Formal analysis, Writing - original draft, Writing - review & editing, Visualization, Data curation. **Gabrielle Boisramé:** Methodology, Formal analysis, Validation, Writing - review & editing. **Scott L. Stephens:** Supervision, Project administration, Writing - review & editing. **Sally Thompson:** Conceptualization, Methodology, Writing - original draft, Funding acquisition, Supervision, Project administration.

Declaration of Competing Interest

The authors declare the following financial interests/personal relationships which may be considered as potential competing interests: We must disclose one conflict of interest: Sally Thompson, senior author on this manuscript, is an editor of the present VSI.

Appendix A. Supplementary data

Supplementary data associated with this article can be found, in the online version, at https://doi.org/10.1016/j.jhydrol.2020.125808.

References

Angrist, J.D., Pischke, J.-S., 2008. Mostly Harmless Econometrics: An Empiricist's Companion. Princeton University Press.

Bart, R.R., Kennedy, M.C., Tague, C.L., McKenzie, D., 2020. Integrating fire effects on vegetation carbon cycling within an ecohydrologic model. Ecological Modelling 416 (108), 880. https://doi.org/10.1016/j.ecolmodel.2019.108880.

Batllori, E., Ackerly, D.D., Moritz, M.A., 2015. A minimal model of fire-vegetation feedbacks and disturbance stochasticity generates alternative stable states in grassland–shrubland–woodland systems. Environmental Research Letters 10 (3), 034,018. https://doi.org/10.1088/1748-9326/10/3/034018.

Batllori, E., Cáceres, M.D., Brotons, L., Ackerly, D.D., Moritz, M.A., Lloret, F., 2018. Compound fire-drought regimes promote ecosystem transitions in mediterranean ecosystems. Journal of Ecology 107 (3), 1187–1198. https://doi.org/10.1111/1365-2745.13115.

Baudena, M., Santana, V.M., Baeza, M.J., Bautista, S., Eppinga, M.B., Hemerik, L., Mayor, A.G., Rodriguez, F., Valdecantos, A., Vallejo, V.R., Vasques, A., Rietkerk, M., 2019. Increased aridity drives post-fire recovery of mediterranean forests towards open shrublands. New Phytologist 225 (4), 1500–1515. https://doi.org/10.1111/nph.16252.

Beven, K., Binley, A., 1992. The future of distributed models: Model calibration and uncertainty prediction. Hydrological Processes 6 (3), 279–298. https://doi.org/10.1002/hyp.3360060305.

Boisramé, G., Thompson, S., Collins, B., Stephens, S., 2017a. Managed wildfire effects on forest resilience and water in the Sierra Nevada. Ecosystems 20 (4), 717–732. https://doi.org/10.1007/s10021-016-0048-1.
Boisramé, G., Thompson, S., Kelly, M., Cavalli, J., Wilkin, K., Stephens, S.L., 2017b. Vegetation change during 40 years of repeated managed wildfires in the Sierra Nevada, California. Forest Ecology and Management 402, 241–252.
Boisramé, G., Thompson, S., Stephens, S., 2018. Hydrologic responses to restored wildfire regimes revealed by soil moisture-vegetation relationships. Advances in Water Resources 112, 124–146. https://doi.org/10.1016/j.advwatres.2017.12.009.
Boisramé, G.F.S., Thompson, S.E., Tague, C.N., Stephens, S.L., 2019. Restoring a natural fire regime alters the water balance of a Sierra Nevada catchment. Water Resources Research 55 (7), 5751–5769. https://doi.org/10.1029/2018wr024098.
Brotons, L., Duane, A., 2019. Correspondence: Uncertainty in climate-vegetation feedbacks on fire regimes challenges reliable long-term projections of burnt area from correlative models. Fire 2 (1), 8. https://doi.org/10.3390/fire2010008.
Burles, K., Boon, S., 2011. Snowmelt energy balance in a burned forest plot, Crowsnest Pass, Alberta, Canada. Hydrological Processes. https://doi.org/10.1002/hyp.8067.
CalFire (2019), Top 20 deadliest CA wildfires, URL:https://www.fire.ca.gov/media/5512/top20_deadliest.pdf, (Accessed on 12/11/2019).
CalFire (2019), Top 20 destructive California wildfires, URL:https://www.fire.ca.gov/media/5511/top20_destruction.pdf, (Accessed on 12/11/2019).
CalFire (2019), Emergency fund fire suppression expenditures, URL:https://www.fire.ca.gov/media/8641/suppressioncostsonepage1.pdf, (Accessed on 12/11/2019).
California Department of Food and Agriculture (2019), California Agricultural Statistics Review 2018–19, pp. 1–121.
Campos, B., Burnett, R., Steel, Z., 2017. Bird and bat inventories in the storrie and chips fire areas 2015–2016: Final report to the lassen national forest.
Cannon, A.J., Sobie, S.R., Murdock, T.Q., 2015. Bias correction of GCM precipitation by quantile mapping: How well do methods preserve changes in quantiles and extremes? Journal of Climate 28 (17), 6938–6959. https://doi.org/10.1175/JCLI-D-14-00754.1.
Collins, B.M., Stephens, S.L., 2007. Managing natural wildfires in Sierra Nevada wilderness areas. Frontiers in Ecology and the Environment 5 (10), 523–527. https://doi.org/10.1890/070007.
Collins, B.M., Miller, J.D., Thode, A.E., Kelly, M., van Wagtendonk, J.W., Stephens, S.L., 2009. Interactions among wildland fires in a long-established Sierra Nevada natural fire area. Ecosystems 12 (1), 114–128. https://doi.org/10.1007/s10021-008-9211-7.
Cornwell, W.K., Stuart, S.A., Ramirez, A., Dolanc, C.R., Thorne, J.H., Ackerly, D.D., 2012. Climate Change Impacts on California Vegetation: Physiology, Life History, and Ecosystem Change. Information Center for the Environment, UC Davis.
Dahm, C.N., Candelaria-Ley, R.I., Reale, C.S., Reale, J.K., Horn, D.J.V., 2015. Extreme water quality degradation following a catastrophic forest fire. Freshwater Biology 60 (12), 2584–2599. https://doi.org/10.1111/fwb.12548.
Davis, K.T., Dobrowski, S.Z., Higuera, P.E., Holden, Z.A., Veblen, T.T., Rother, M.T., Parks, S.A., Sala, A., Maneta, M.P., 2019. Wildfires and climate change push low-elevation forests across a critical climate threshold for tree regeneration. Proceedings of the National Academy of Sciences 116 (13), 6193–6198. https://doi.org/10.1073/pnas.1815107116.
Dettinger, M.D., 2005. From climate-change spaghetti to climate-change distributions for 21st century California, San Francisco Estuary and Watershed. Science 3 (1). https://doi.org/10.15447/sfews.2005v3iss1art6.
Doerr, S., Shakesby, R., Blake, W., Chafer, C., Humphreys, G., Wallbrink, P., 2006. Effects of differing wildfire severities on soil wettability and implications for hydrological response. Journal of Hydrology 319 (1–4), 295–311. https://doi.org/10.1016/j.jhydrol.2005.06.038.
Ebel, B.A., Moody, J.A., 2020. Parameter estimation for multiple post-wildfire hydrologic models. Hydrological Processes. https://doi.org/10.1002/hyp.13865.
Geos Institute. 2013. Future climate, wildfire, hydrology, and vegetation projections for the sierra nevada, California: A climate change synthesis in support of the vulnerability assessment/adaptation strategy process., online: https://climatewise.org/images/projects/sierra-nevada-report-projections.pdf.
Gleason, K.E., Nolin, A.W., Roth, T.R., 2013. Charred forests increase snowmelt: Effects of burned woody debris and incoming solar radiation on snow ablation. Geophysical Research Letters 40 (17), 4654–4661. https://doi.org/10.1002/grl.50896.
Gleason, K.E., McConnell, J.R., Arienzo, M.M., Chellman, N., Calvin, W.M., 2019. Four-fold increase in solar forcing on snow in western u.s. burned forests since 1999. Nature Communications 10 (1). https://doi.org/10.1038/s41467-019-09935-y.
González-Sanchis, M., Ruiz-Pérez, G., Campo, A.D.D., Garcia-Prats, A., Francés, F., Lull, C., 2019. Managing low productive forests at catchment scale: Considering water, biomass and fire risk to achieve economic feasibility. Journal of Environmental Management 231, 653–665. https://doi.org/10.1016/j.jenvman.2018.10.078.
Goulden, M., Bales, R., 2019. California forest die-off linked to multi-year deep soil drying in 2012–2015 drought. Nature Geoscience 1. https://doi.org/10.1038/s41561-019-0388-5.
Green, W.H., Ampt, G., 1911. Studies on soil physics. The Journal of Agricultural Science 4 (1), 1–24.
Hagedorn, R., Doblas-Reyes, F.J., Palmer, T., 2005. The rationale behind the success of multi-model ensembles in seasonal forecasting — i. basic concept. Tellus A: Dynamic Meteorology and Oceanography 57 (3), 219–233. https://doi.org/10.3402/tellusa.v57i3.14657.
Halofsky, J.S., Conklin, D.R., Donato, D.C., Halofsky, J.E., Kim, J.B., 2018. Climate change, wildfire, and vegetation shifts in a high-inertia forest landscape: Western washington, u.s.a. PLOS ONE 13 (12). https://doi.org/10.1371/journal.pone.0209490 e0209,490.
Henn, B., Clark, M.P., Kavetski, D., Newman, A.J., Hughes, M., McGurk, B., Lundquist, J. D., 2018. Spatiotemporal patterns of precipitation inferred from streamflow observations across the Sierra Nevada mountain range. Journal of Hydrology 556, 993–1012. https://doi.org/10.1016/j.jhydrol.2016.08.009.
Her, Y., Yoo, S.-H., Cho, J., Hwang, S., Jeong, J., Seong, C., 2019. Uncertainty in hydrological analysis of climate change: multi-parameter vs. multi-GCM ensemble predictions. Scientific Reports 9 (1). https://doi.org/10.1038/s41598-019-41334-7.
Hurteau, M.D., Liang, S., Westerling, A.L., Wiedinmyer, C., 2019. Vegetation-fire feedback reduces projected area burned under climate change. Scientific Reports 9 (1). https://doi.org/10.1038/s41598-019-39284-1.
Kane, V.R., Lutz, J.A., Cansler, C.A., Povak, N.A., Churchill, D.J., Smith, D.F., Kane, J.T., North, M.P., 2015. Water balance and topography predict fire and forest structure patterns. Forest Ecology and Management 338, 1–13. https://doi.org/10.1016/j.foreco.2014.10.038.
Kennedy, M.C., McKenzie, D., Tague, C., Dugger, A.L., 2017. Balancing uncertainty and complexity to incorporate fire spread in an eco-hydrological model. International Journal of Wildland Fire 26 (8), 706. https://doi.org/10.1071/wf16169.
Klausmeyer, K., Fitzgerald, K., 2012. Where Does California's Water Come From? Land conservation and the watersheds that supply California's drinking water, online: https://www.nature.org/media/california/california_drinking-water-sources-2012.pdf.
Kostadinov, T.S., Schumer, R., Hausner, M., Bormann, K.J., Gaffney, R., McGwire, K., Painter, T.H., Tyler, S., Harpold, A.A., 2019. Watershed-scale mapping of fractional snow cover under conifer forest canopy using lidar. Remote Sensing of Environment 222, 34–49. https://doi.org/10.1016/j.rse.2018.11.037.
Lanzante, J.R., Adams-Smith, D., Dixon, K.W., Nath, M., Whitlock, C.E., 2019. Evaluation of some distributional downscaling methods as applied to daily maximum temperature with emphasis on extremes. International Journal of Climatology. https://doi.org/10.1002/joc.6288.
Larsen, I.J., MacDonald, L.H., Brown, E., Rough, D., Welsh, M.J., Pietraszek, J.H., Libohova, Z., de Dios Benavides-Solorio, J., Schaffrath, K., 2009. Causes of post-fire runoff and erosion: water repellency, cover, or soil sealing? Soil Science Society of America Journal 73 (4), 1393–1407.
Lauvaux, C.A., Skinner, C.N., Taylor, A.H., 2016. High severity fire and mixed conifer forest-chaparral dynamics in the southern Cascade Range, USA. Forest Ecology and Management 363, 74–85. https://doi.org/10.1016/j.foreco.2015.12.016.
Lenihan, J.M., Drapek, R., Bachelet, D., Neilson, R.P., 2003. Climate change effects on vegetation distribution, carbon, and fire in California. Ecological Applications 13 (6), 1667–1681. https://doi.org/10.1890/025295.
Liang, S., Hurteau, M.D., Westerling, A.L., 2016. Response of Sierra Nevada forests to projected climate-wildfire interactions. Global Change Biology 23 (5), 2016–2030. https://doi.org/10.1111/gcb.13544.
Littell, J.S., McKenzie, D., Peterson, D.L., Westerling, A.L., 2009. Climate and wildfire area burned in western us ecoprovinces, 1916–2003. Ecological Applications 19 (4), 1003–1021.
Lundquist, J.D., Dickerson-Lange, S.E., Lutz, J.A., Cristea, N.C., 2013. Lower forest density enhances snow retention in regions with warmer winters: A global framework developed from plot-scale observations and modeling. Water Resources Research 49 (10), 6356–6370. https://doi.org/10.1002/wrcr.20504.
Luo, M., Liu, T., Meng, F., Duan, Y., Frankl, A., Bao, A., Maeyer, P.D., 2018. Comparing bias correction methods used in downscaling precipitation and temperature from regional climate models: A case study from the Kaidu River Basin in Western China. Water 10 (8), 1046. https://doi.org/10.3390/w10081046.
Madani, K., Lund, J.R., 2009. Estimated impacts of climate warming on California's high-elevation hydropower. Climatic Change 102 (3–4), 521–538. https://doi.org/10.1007/s10584-009-9750-8.
Maina, F.Z., Siirila-Woodburn, E.R., 2019. Watersheds dynamics following wildfires: Nonlinear feedbacks and implications on hydrologic responses. Hydrological Processes 34 (1), 33–50. https://doi.org/10.1002/hyp.13568.
McKenzie, D., Littell, J.S., 2017. Climate change and the eco-hydrology of fire: Will area burned increase in a warming western USA? Ecological Applications 27 (1), 26–36.
Meng, R., Dennison, P.E., Huang, C., Moritz, M.A., D'Antonio, C., 2015. Effects of fire severity and post-fire climate on short-term vegetation recovery of mixed-conifer and red fir forests in the Sierra Nevada mountains of California. Remote Sensing of Environment 171, 311–325. https://doi.org/10.1016/j.rse.2015.10.024.
Millar, C.I., Stephenson, N.L., 2015. Temperate forest health in an era of emerging megadisturbance. Science 349 (6250), 823–826. https://doi.org/10.1126/science.aaa9933.
Miller, J.D., Thode, A.E., 2007. Quantifying burn severity in a heterogeneous landscape with a relative version of the delta normalized burn ratio (dNBR). Remote Sensing of Environment 109 (1), 66–80. https://doi.org/10.1016/j.rse.2006.12.006.
Monteith, J.L., 1965. Evaporation and environment, in Symposia of the society for experimental biology, vol. 19. Cambridge University Press (CUP) Cambridge, pp. 205–234.
Najafi, M.R., Moradkhani, H., Jung, I.W., 2011. Assessing the uncertainties of hydrologic model selection in climate change impact studies. Hydrological Processes 25 (18), 2814–2826. https://doi.org/10.1002/hyp.8043.
Neary, D.G., Ryan, K.C., DeBano, L.F., 2005. Wildland Fire in Ecosystems, effects of fire on soil and water, USDA-FS general technical report, 4(September), 250, doi: https://doi.org/10.1111/j.1467-7717.2009.01106.x.
Pierce, D.W., Barnett, T.P., Santer, B.D., Gleckler, P.J., 2009. Selecting global climate models for regional climate change studies. Proceedings of the National Academy of Sciences 21, 8441–8446. https://doi.org/10.1073/pnas.0900094106.
Pierce, D.W., Cayan, D.R., Das, T., Maurer, E.P., Miller, N.L., Bao, Y., Kanamitsu, M., Yoshimura, K., Snyder, M.A., Sloan, L.C., Franco, G., Tyree, M., 2013. The key role of heavy precipitation events in climate model disagreements of future annual

precipitation changes in California. Journal of Climate 26 (16), 5879–5896. https://doi.org/10.1175/jcli-d-12-00766.1.
Ponisio, L.C., Wilkin, K., M'Gonigle, L.K., Kulhanek, K., Cook, L., Thorp, R., Griswold, T., Kremen, C., 2016. Pyrodiversity begets plant–pollinator community diversity. Global Change Biology 22 (5), 1794–1808.
Richter, C., Rejmánek, M., Miller, J.E.D., Welch, K.R., Weeks, J., Safford, H., 2019. The species diversity × fire severity relationship is hump-shaped in semiarid yellow pine and mixed conifer forests. Ecosphere 10 (10). https://doi.org/10.1002/ecs2.2882.
Riley, K.L., Loehman, R.A., 2016. Mid-21st-century climate changes increase predicted fire occurrence and fire season length, Northern Rocky Mountains, United States. Ecosphere 7 (11). https://doi.org/10.1002/ecs2.1543.
Riley, K.L., Williams, A.P., Urbanski, S.P., Calkin, D.E., Short, K.C., O'Connor, C.D., 2019. Will landscape fire increase in the future? a systems approach to climate, fire, fuel, and human drivers. Current Pollution Reports 5 (2), 9–24. https://doi.org/10.1007/s40726-019-0103-6.
Sanderson, B.M., Wehner, M., Knutti, R., 2017. Skill and independence weighting for multi-model assessments. Geoscientific Model Development 10 (6), 2379–2395. https://doi.org/10.5194/gmd-10-2379-2017.
Scholl, A.E., Taylor, A.H., 2010. Fire regimes, forest change, and self-organization in an old-growth mixed-conifer forest, Yosemite National Park, USA. Ecological Applications 20 (2), 362–380. https://doi.org/10.1890/08-2324.1.
Serra-Diaz, J.M., Maxwell, C., Lucash, M.S., Scheller, R.M., Laflower, D.M., Miller, A.D., Tepley, A.J., Epstein, H.E., Anderson-Teixeira, K.J., Thompson, J.R., 2018. Disequilibrium of fire-prone forests sets the stage for a rapid decline in conifer dominance during the 21st century. Scientific Reports 8 (1). https://doi.org/10.1038/s41598-018-24642-2.
Smith, H.G., Sheridan, G.J., Lane, P.N., Nyman, P., Haydon, S., 2011. Wildfire effects on water quality in forest catchments: A review with implications for water supply. Journal of Hydrology 396 (1–2), 170–192. https://doi.org/10.1016/j.jhydrol.2010.10.043.
Steel, Z.L., Safford, H.D., Viers, J.H., 2015. The fire frequency-severity relationship and the legacy of fire suppression in California forests. Ecosphere 6 (1). https://doi.org/10.1890/es14-00224.1 art8.
Stephens, S.L., Lydersen, J.M., Collins, B.M., Fry, D.L., Meyer, M.D., 2015. Historical and current landscape-scale ponderosa pine and mixed conifer forest structure in the southern Sierra Nevada. Ecosphere 6 (5). https://doi.org/10.1890/es14-00379.1 art9.
Stephens, S.L., Collins, B.M., Biber, E., Fulé, P.Z., 2016. U.S. federal fire and forest policy: emphasizing resilience in dry forests. Ecosphere 7 (11). https://doi.org/10.1002/ecs2.1584 e01,584.
Stephens, S.L., Kobziar, L.N., Collins, B.M., Davis, R., Fulé, P.Z., Gaines, W., Ganey, J., Guldin, J.M., Hessburg, P.F., Hiers, K., Hoagland, S., Keane, J.J., Masters, R.E., McKellar, A.E., Montague, W., North, M., Spies, T.A., 2019. Is fire "for the birds? how two rare species influence fire management across the US. Frontiers in Ecology and the Environment 17 (7), 391–399. https://doi.org/10.1002/fee.2076.
Stephens, S.L., Westerling, A.L., Hurteau, M.D., Peery, M.Z., Schultz, C.A., Thompson, S., 2020. Fire and climate change: conserving seasonally dry forests is still possible. Frontiers in Ecology and the Environment 18, 354–360. https://doi.org/10.1002/fee.2218.
Stevens, J.T., 2017. Scale-dependent effects of post-fire canopy cover on snowpack depth in montane coniferous forests. Ecological Applications 27 (6), 1888–1900. https://doi.org/10.1002/eap.1575.
Stevens, J.T., Boisramé, G.F.S., Rakhmatulina, E., Thompson, S.E., Collins, B.M., Stephens, S.L., 2020. Forest vegetation change and its impacts on soil water following 47 years of managed wildfire. Ecosystems. https://doi.org/10.1007/s10021-020-00489-5.
Syphard, A.D., Sheehan, T., Rustigian-Romsos, H., Ferschweiler, K., 2018. Mapping future fire probability under climate change: Does vegetation matter? PLOS ONE 13 (8). https://doi.org/10.1371/journal.pone.0201680 e0201,680.
Tague, C.L., Band, L.E., 2004. RHESSys: Regional hydro-ecologic simulation system-an object-oriented approach to spatially distributed modeling of carbon, water, and nutrient cycling. Earth Interactions 8 (19), 1–42. https://doi.org/10.1175/1087-3562(2004)8<1:RRHSSO>2.0.CO;2.
Tague, C.L., Moritz, M., Hanan, E., 2019. The changing water cycle: The eco-hydrologic impacts of forest density reduction in mediterranean (seasonally dry) regions. Wiley Interdisciplinary Reviews: Water, e1350. https://doi.org/10.1002/wat2.1350.
Tarroja, B., AghaKouchak, A., Samuelsen, S., 2016. Quantifying climate change impacts on hydropower generation and implications on electric grid greenhouse gas emissions and operation. Energy 111, 295–305. https://doi.org/10.1016/j.energy.2016.05.131.
Thomas, D., Butry, D., Gilbert, S., Webb, D., Fung, J., 2017. The costs and losses of wildfires: a literature survey, Tech. rep., doi: 10.6028/nist.sp.1215.
Thompson, P.D., 1977. How to improve accuracy by combining independent forecasts. Monthly Weather Review 105 (2), 228–229. https://doi.org/10.1175/1520-0493(1977)105<0228:HTIABC>2.0.CO;2.
Tiedemann, A.R., Conrad, C.E., Dieterich, J.H., Hornbeck, J.W., Megahan, W.S., Viereck, L.A., Wade, D.D., 1979. Effects of fire on water: a state of knowledge review, p. 28.
van Wagtendonk, J.W., 2007. The history and evolution of wildland fire use. Fire Ecology 3 (2), 3–17. https://doi.org/10.4996/fireecology.0302003.
van Wagtendonk, J.W., van Wagtendonk, K.A., Thode, A.E., 2012. Factors associated with the severity of intersecting fires in Yosemite national park, California, USA. Fire Ecology 7 (1), 11–31. https://doi.org/10.4996/fireecology.0801011.
Westerling, A.L. (2018), Wildfire simulations for California's fourth climate change assessment: Projecting changes in extreme wildfire events with a warming climate, pp. 1–29, online: https://www.energy.ca.gov/sites/default/files/2019-11/Projections_CCCA4-CEC-2018-014_ADA.pdf.
Westerling, A.L., Bryant, B.P., 2008. Climate change and wildfire in California. Climatic Change 87 (1), 231–249. https://doi.org/10.1007/s10584-007-9363-z.
Wine, M.L., Cadol, D., Makhnin, O., 2018. In ecoregions across western USA streamflow increases during post-wildfire recovery. Environmental Research Letters 13 (1), 014,010. https://doi.org/10.1088/1748-9326/aa9c5a.
Wood, C.M., Jones, G.M., 2019. Framing management of social-ecological systems in terms of the cost of failure: the Sierra Nevada, USA as a case study. Environmental Research Letters 14 (10), 105,004. https://doi.org/10.1088/1748-9326/ab4033.
Writer, J.H., Hohner, A., Oropeza, J., Schmidt, A., Cawley, K.M., Rosario-Ortiz, F.L., 2014. Water treatment implications after the High Park Wildfire, Colorado. Journal – American Water Works Association 106 (4), E189–E199. https://doi.org/10.5942/jawwa.2014.106.0055.
Young, D.J.N., Werner, C.M., Welch, K.R., Young, T.P., Safford, H.D., Latimer, A.M., 2019. Post-fire forest regeneration shows limited climate tracking and potential for drought-induced type conversion. Ecology 100 (2). https://doi.org/10.1002/ecy.2571 e02,571.
Yue, X., Mickley, L.J., Logan, J.A., 2013. Projection of wildfire activity in southern California in the mid-twenty-first century. Climate Dynamics 43 (7–8), 1973–1991. https://doi.org/10.1007/s00382-013-2022-3.